Poly(L-lactic acid) Nanocomposites with Layered Double Hydroxides Functionalized with Ibuprofen

Koffi L. Dagnon,[1] Sriram Ambadapadi,[2] Ali Shaito,[1] Sunny M. Ogbomo,[1] Vallerie DeLeon,[2] Teresa D. Golden,[2] Maham Rahimi,[3] Kytai Nguyen,[3] Paul S. Braterman,[4] Nandika Anne D'Souza[1]

[1]*Department of Materials Science and Engineering, University of North Texas, P.O. Box 305310, Denton, Texas 76205*
[2]*Department of Chemistry, University of North Texas, P.O. Box 305070, Denton, Texas 76203*
[3]*Department of Bioengineering, University of Texas at Arlington, P.O. Box 19138, Arlington, Texas 76019*
[4]*Department of Chemistry, University of Glasgow, Glasgow G128QQ, Scotland*

Received 29 October 2008; accepted 29 January 2009
DOI 10.1002/app.30159
Published online 17 April 2009 in Wiley InterScience (www.interscience.wiley.com).

ABSTRACT: The detrimental effect of cell adhesion on polymer surfaces has been a limiting factor in the medical deployment of many implants. We examined the potential to decrease cell proliferation while simultaneously increasing mechanical performance through Zn–Al layered double hydroxide (LDH) organically modified with ibuprofen dispersed in poly(L-lactic acid) (PLLA). These composites are commonly referred to as *nanocomposites.* The thermophysical and mechanical properties of the hybrids were studied with wide-angle X-ray diffraction (WAXD), transmission electron microscopy (TEM), differential scanning calorimetry, thermogravimetric analysis, dynamic mechanical analysis, and tensile testing. The WAXD and TEM results indicated that intercalated and exfoliated nanocomposites were obtained. The storage modulus, tensile modulus, and ultimate tensile strength were improved. The LDH affected the cold crystallization and reduced the thermal stability of the neat PLLA. Smooth muscle cells were used for *in vitro* studies of the nanocomposites. It was found that the hybrids reduced cell proliferation, and the amount of cell reduction was related to ibuprofen release. © 2009 Wiley Periodicals, Inc. J Appl Polym Sci 113: 1905–1915, 2009

Key words: biomaterials; biopolymers; mechanical properties; nanocomposites; thermal properties

INTRODUCTION

Synthetic materials are increasingly being used in clinics and hospitals for surgical sutures, in guided tissue regeneration,[1–3] as bone filler,[4,5] and in drug-delivery systems.[6–9] The deployment of biopolymers such as poly(L-lactic acid) (PLLA) as implants in the body has been an area of some concern.[10] Concerns include possible inflammation of the tissue around the biopolymers leading to increased cell adhesion and decreased mechanical performance of the implant. Decreased cell proliferation has been found in previous efforts based on the incorporation of drugs into inorganic materials such as montmorillonite and layered double hydroxide (LDH) clays.[11–13] The biocompatibility of the LDHs[14–16] makes them an ideal choice for safe drug delivery. The use of polymers as hosts for drug delivery has also been of considerable interest. In particular, studies of bioimplants with ibuprofen-modified poly(L-lactic acid) (PLLA/Ibu) have shown that ibuprofen inhibits the smooth muscle cell (SMC) proliferation and have demonstrated ibuprofen's role in reducing implant-associated restenosis in arteries.[17]

Clays have also been found to increase the mechanical properties of polymers. Nanocomposites based on the dispersion of smectite clays have proven to be particularly useful because improved mechanical properties can be obtained with the addition of a few percentages by weight.[18] The driving parameter for improved mechanical performance is the enhanced interfacial area afforded by the expansion and dispersion of nanoplates in the medium. The nanoplates can either be cation exchanging or anion exchanging. Montmorillonite, for instance, is a commonly investigated cation-exchanged clay. LDHs have the general formula $[M^{II}_{1-x}M^{III}_{x}(OH)_{2x}]^{x+}(A^{n-})_{x/n}\cdot mH_2O$, where M^{II} represents a divalent metal, M^{III} represents a trivalent metal, and A^{n-} represents an anion. They have a brucite-like structure, in which a fraction of the divalent metal is replaced with a trivalent metal. The replacement gives the layers a positive charge, and anions are intercalated between these layers to maintain the electroneutrality.[19,20] The intercalation of organic compounds into the LDHs provides a useful synthetic route for preparing organic–inorganic hybrids that contain properties of both the organic guest and the inorganic host in a single material.[21]

Correspondence to: N. A. D'Souza (ndsouza@unt.edu).

The resulting properties can be tailored to specific requirements needed to serve specific purposes.

The dual functionality of decreased cell proliferation and enhanced mechanical properties may be possible if the LDH is functionalized by nonsteroidal anti-inflammatory drugs such as ibuprofen. In this article, we present the possibility of using nanoclay fillers functionalized with a nonsteroidal anti-inflammatory drug (ibuprofen) for a combined benefit of decreased cell adhesion and improved mechanical performance. No study of layered double hydroxide ibuprofen (LDH Ibu) with PLLA nanocomposite has been reported to our knowledge. Films were spun-cast, and the dispersion, thermophysical characterization, cell proliferation, and drug-release measurements were conducted with various analytical methods.

EXPERIMENTAL

Materials

PLLA (number-average molecular weight = 98,600 Da and weight-average molecular weight = 194,799 Da) was supplied by NatureWorks LLC (Minnetonka, MN) and was dried in oven for 48 h at 35°C. Dichloromethane (>99.8% purity, EMD, Chemicals, Gibbstown, NJ), sodium hydroxide (50% NaOH solution, Sigma–Aldrich, St. Louis, MO), aluminum nitrate hexahydrate [$Al(NO_3)_3{\cdot}6H_2O$, Alfa Aesar, Ward Hill, MA], zinc nitrate hexahydrate [$Zn(NO_3)_2{\cdot}6H_2O$, Alfa Aesar], and sodium salt of ibuprofen (Ibu; Sigma-Aldrich, St. Louis, MO) were used as received for the synthesis of different LDHs.

Preparation of the Zn–Al LDH nitrate (LDH NO_3)

To prepare 2 g of 2 : 1 Zn–Al LDH NO_3, 4.08 g of $Al(NO_3)_3{\cdot}6H_2O$ and 11.87 g of $Zn(NO_3)_2{\cdot}6H_2O$ were dissolved in 133 mL of freshly drawn deionized water (Millipore MilliQ Academic, Billerica, MA, 18.2 MΩ/cm). The solution was neutralized with 4.2 mL of NaOH to precipitate the 2 : 1 Zn–Al LDH NO_3. The water used for the preparation of the Zn–Al LDH NO_3 was heated to around 40°C before the metal nitrates and sodium hydroxide were added, and the mixture was stirred constantly under a stream of nitrogen gas to minimize the absorption of CO_2. The precipitate was then aged in the mother liquor for 24 h at a temperature of about 90–100°C under a nitrogen gas blanket, after which it was allowed to cool and centrifuged to separate the precipitate. It was washed two more times with deionized water to remove any remaining ions from the mother liquor. This crystalline white solid, designated as LDH NO_3, was used for the exchange with Ibu. A nitrate precursor was made because the nitrate anion is easier to exchange with the desired anion, ibuprofen here, than with other general choices such as chloride and carbonate.

Preparation of the Zn–Al LDH Ibu

A solution of Ibu (3.64 g in 50 mL of deionized water) was added to a suspension of the nitrate precursor prepared as described previously. The mixture was stirred under a nitrogen gas blanket for 1 h before the precipitate was separated and washed twice with deionized water by centrifugation. The molar ratio of the Ibu to the LDH NO_3 was 1 : 2. This slight excess, in the place of 1 : 1, was used to facilitate anion exchange. The crystalline white solid thus obtained was dried in a hot-air oven at 70°C and was designated as LDH Ibu.

Preparation of the PLLA/LDH Ibu nanocomposites

The nanocomposites were prepared by the solution casting route. Initially, the LDH Ibu powder was dispersed in 75 mL of dichloromethane and stirred for 10 min. Then, 3.0 g of PLLA was added, and the mixture was heated at 40°C under vigorous stirring for 4 h. The resulting dispersion was allowed to age for 24 h. Nanocomposite films were prepared by spin casting (with a custom-built spin caster without the need for any substrate), and the samples were dried *in vacuo* at 35°C for 4 days to remove residual solvent. The LDH Ibu amounts corresponded to effective weight percentages of 1, 3, and 5% nanocomposite, which are referred to as 1LDH Ibu, 3LDH Ibu, and 5LDH Ibu, respectively. For the cell proliferation measurements, 1 mL of the resulting dispersion was collected in several cylindrical glass vials specially made with a volume capacity of about 2 mL. The solvent was allowed to evaporate from the vials; this left a thin film of PLLA/LDH Ibu nanocomposite. Control samples of PLLA and PLLA/Ibu were also prepared as needed for control experiments.

Metals and CHN analyses of the LDH Ibu

The metals analysis was conducted on the LDH NO_3 and LDH Ibu samples with a PerkinElmer Analyst 300 (Waltham, MA) with PerkinElmer supplied standards and element lamps. The sample was dissolved in a 5% HNO_3 solution. The CHN analysis was performed by Elf Analytical Services, Inc. (Ocean, NJ).

Fourier transform infrared (FTIR) analysis

To ensure that the nitrate anions were successfully exchanged by ibuprofen anions, FTIR measurements of the LDH NO_3, LDH Ibu, and Ibu samples were performed with a Nicolet Nexus 6700 FTIR

spectrometer (Thermo Fisher Scientific Inc., Waltham, MA) with a resolution of 4 cm^{-1} and a scan range of 4000–400 cm^{-1}. A total of 64 scans per sample were performed.

Wide-angle X-ray diffraction (WAXD) analysis

To confirm the success of the functionalization process, WAXD measurement was conducted on the LDH NO_3 and LDH Ibu samples. WAXD measurement was also conducted on the PLLA/LDH Ibu nanocomposites to study the dispersion of the nanofiller in the PLLA matrix. For all samples, diffractograms were obtained with a Rigaku model D/Max Ultima III X-ray diffractometer (Woodlands, TX). Each sample was scanned from 2 to 70° (2θ) with a step size of 0.05° and a dwell time of 1.34 s with Cu Kα radiation (λ = 1.540562 Å, generated at 44 mA and 40 kV).

Transmission electron microscopy (TEM) analysis

TEM was used to complement the WAXD results on the nanoplatelet dispersion. Brightfield TEM images were recorded on Philips EM 420 (Mahwah, NJ) equipment at an accelerating voltage of 120 kV. Before the analysis, samples of PLLA/LDH Ibu nanocomposites were sandwiched and glued between two sheets of epoxy resin. The sandwiched samples were then cut into slices of a nominal thickness of 90 nm with a diamond knife on an RMC MT 6000 (Tucson, AZ) ultra microtome at room temperature. The sections were transferred from water at room temperature onto a 200-mesh copper grid.

Thermogravimetric analysis (TGA)

The thermal stability of the neat LDH Ibu, neat Ibu, neat PLLA, and nanocomposites was measured with a PerkinElmer TGA6. Around 15 mg of each sample was weighed in a standard ceramic pan and run under a nitrogen atmosphere. The measurements were taken from 30 to 700°C at 10°C/min. All TGA measurements were done in duplicate.

Differential scanning calorimetry (DSC) measurement

The thermal properties of the parent PLLA and nanocomposites were recorded on a DSC 6 PerkinElmer apparatus under a nitrogen atmosphere. The system was calibrated with elemental indium. The samples were run from 30 to 200°C, held at 200°C for 5 min to erase their thermal history, and then cooled to 30°C. The heating and cooling rates were maintained at 10°C/min. Two runs were conducted, and each sample was tested in duplicate.

Dynamic mechanical analysis (DMA)

The viscoelastic properties of the parent PLLA and its nanocomposites were measured with a dynamical mechanical analyzer RSA III (TA Instruments, New Castle, DE), operating in the tensile mode. The mean sample dimensions were 25 × 5 mm^2 with a mean thickness of 0.15 ± 0.01 mm. Samples were scanned from −50 to 100°C at a heating rate of 3°C/min, a frequency of 1 Hz, and a strain amplitude of 0.25% (determined from a separate strain amplitude sweep at 1 Hz to establish the linear viscoelastic region). All dynamic mechanical analysis measurements were done in triplicate.

Tensile testing

The tensile properties of the neat PLLA and its nanocomposites were measured with the Rheometric Solids Analyzer 3 dynamical mechanical analyzer RSA III (TA Instruments), operating in the tensile mode with a strain rate of 0.04 min^{-1}. Three samples with dimensions of 25 × 5 mm^2 and a thickness of 0.15 ± 0.01 mm were taken to get the average tensile properties.

Smooth muscle cell (SMC) proliferation studies

Human aortic SMCs obtained from Invitrogen (Carlsbad, CA) were cultured in a complete medium consisting of Dulbecco's Modified Eagle Medium supplemented with 10% fetal bovine serum and 1% penicillin/streptomycin. Cells were incubated in a humid environment at 37°C and 5% CO_2. Upon 80–90% confluence, the cells were passaged or used for experiments. Cells up to passage 9 were used in the experiments. Before cell studies, all glass sample vials were sterilized under UV radiation for 30 min. For the proliferation studies, SMCs were harvested after trypsinization from culture flasks and seeded onto plain glass vials (controls) and glass vials containing pure PLLA; 1, 3, or 5 wt % PLLA/LDH Ibu; PLLA/Ibu; LDH Ibu; or Ibu samples at an approximate seeding density of 9000 cells/cm^2. After 5 days of seeding, the cells were washed with phosphate-buffered saline (PBS) and then lysed with 1 mL of 1% Triton X-100 for 30 min at 37°C. We determined the concentration of total cell sample DNA (μg of DNA/mL) as an equivalent to the cell number or the number of proliferation cells with PicoGreen DNA assay kits (Molecular Probes, Eugene, OR) following the manufacturer's instructions.

Statistical analysis

Analysis of the results was performed with analysis of variance with post hoc comparisons (StatView 5.0

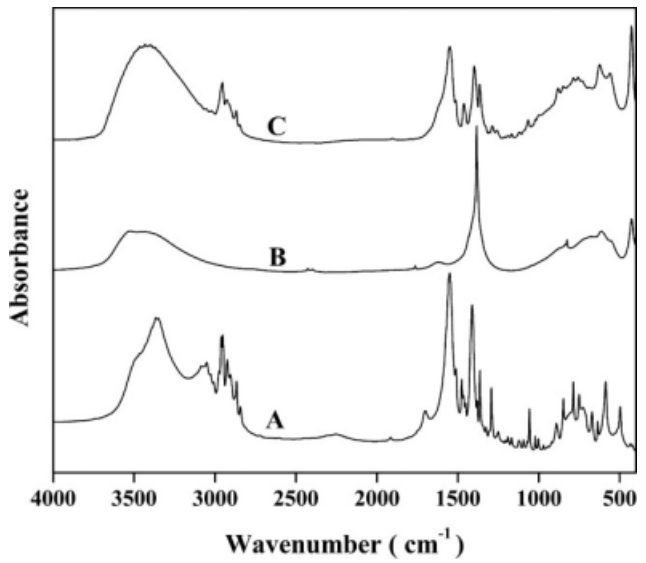

Figure 1 FTIR spectra of (A) Ibu, (B) LDH NO_3, and (C) LDH Ibu.

software, SAS Institute, Cary, NC). For each study, the sample size was 4 ($n = 4$), and all of the results are presented as Mean ± Standard deviation. The results are considered significantly different with $p < 0.05$.

High-performance liquid chromatography (HPLC) drug release

Drug-release experiments were performed with HPLC (Thermo Scientific's Finnigan Surveyor). The PLLA/Ibu and PLLA/LDH Ibu films (35 × 20 mm^2) were placed in glass vials and incubated 37°C with PBS with a pH of 7.4. The vials were capped for up to 5 days with mild shaking. At appropriate times, the PBS was collected and replaced with fresh buffer. Triplicate aliquot samples (20 μL of the PBS solution) were injected into the HPLC to determine the Ibu concentration released from the films. The HPLC conditions were as follows: column, Thermo C18 (150 × 4.6 mm); mobile phase, 60 : 40 acetonitrile : 0.1% trifluoracetic acid in water (pH = 2.55); flow rate = 1.5 mL/min; 20-μL injection; and UV–visible detection at 220 nm. Ibuprofen eluted under these HPLC conditions at a retention time of 3.9 min. The peak areas were used to calculate the concentrations of ibuprofen released from the films.

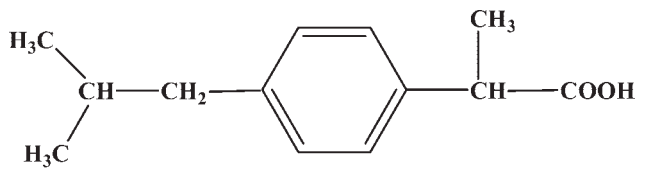

Scheme 1 Chemical structure of ibuprofen.

Triplicate analysis was done for each injection to obtain a relative standard deviation for each point in the Ibu release curves. Modified Freundlich plots of the experimental data matched a diffusion-controlled process for the release of Ibu.

RESULTS AND DISCUSSION

Synthesis of the LDH Ibu and structural characterization

The FTIR spectra of the pure LDH NO_3, Ibu, and pure LDH Ibu are presented in Figure 1. Scheme 1 represents the chemical structure of ibuprofen. The spectrum of the salt[22,23] showed alkyl stretching peaks around 3000–2800 cm^{-1}, carbonyl stretching mode at 1703 cm^{-1}, and the asymmetric and symmetric $RCOO^-$ stretches at 1550 and 1380 cm^{-1}. The peaks around 3380, 1384, and 426 cm^{-1} in the spectrum of the parent nitrate material indicated the presence of nitrate interlayer anions and also confirmed the Zn–Al LDH structure, as did the other broad peaks below 1000 cm^{-1}. The loss of the characteristic nitrate peak (1384 cm^{-1}) and the presence of the ibuprofen anion peaks demonstrated the replacement of nitrate by this anion in the exchanged material. The C—H stretching vibrations at 2963 cm^{-1} showed the presence of the methyl group of the ibuprofen and confirmed the intercalation of the ibuprofen into the Zn–Al LDH layers. The band at 845 cm^{-1} corresponded to the C—H bend (p-substituted for the aromatic group), the absorption band at 1559 cm^{-1} corresponded to C=C stretching, the absorption region between 720 and 725 cm^{-1} corresponded to CH_2 bending of the alkyl

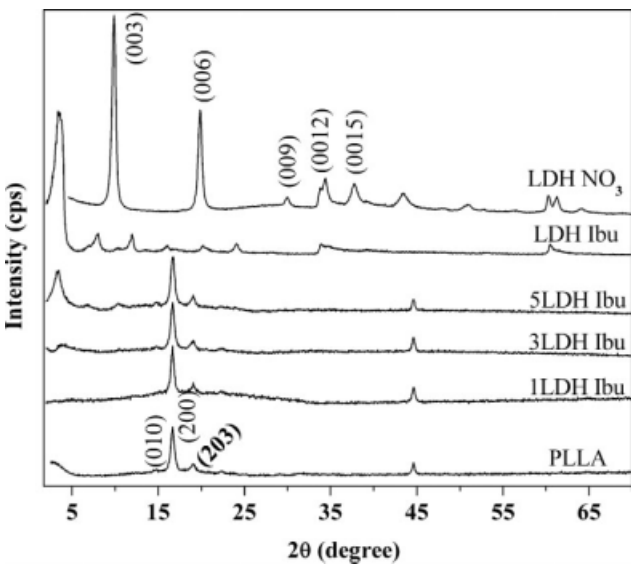

Figure 2 WAXD patterns of the neat LDH NO_3, neat LDH Ibu, neat PLLA, and PLLA/LDH Ibu nanocomposites with different LDH Ibu loadings.

TABLE I
WAXD Characteristic Peaks of LDH Ibu

	(003)	(006)	(009)	(0012)	(0015)	(110/113)
2θ (°)	3.84	7.94	11.94	15.95	20.10	60.50
Interlayer spacing (Å)	22.95	11.11	7.40	5.55	4.41	1.52
fwhm	0.69	0.57	0.58	0.62	0.56	0.80

group for the substituted aromatic group, the absorption region at 744 cm^{-1} corresponded to CH out-of-plane bending of the aromatic ring, and the region from 410 to 500 cm^{-1} corresponded to X—O and O—X—O (X = Mg, Zn, Al, or Cu).[24,25]

The WAXD pattern of the exchanged material LDH Ibu showed an interlayer spacing of 22.95 Å at a 2θ of 3.84° for the (003) reflection peak (Fig. 2). This *d*-spacing showed an increase of approximately 13.94 Å in comparison with the *d*-spacing of the nitrate precursor (shown later in Table II), which confirmed the intercalation of ibuprofen between the layers. The size of the ibuprofen molecule was 10–11 Å, and the *d*-spacing fit well with an interpenetrating double-layer arrangement model of the molecules in the gallery space.[26] The other reflections, (006), (009), and (0012), could also be seen clearly in the pattern, which indicated the superior crystallinity of the material. For each reflection peak of LDH Ibu, the angle (2θ), *d*-spacing, and full width at half-maximum (fwhm) values are given in Table I.

Metal and elemental analyses showed the presence of 25.9% Zn, 5.4% Al, 29.6% C, 5.48% H, and 0.06% N in LDH Ibu. When compared to the theoretical percentages derived from the formula $Zn_2Al(OH)_6(C_{13}H_{17}O_2)\cdot 2H_2O$ of 26.8% Zn, 5.56% Al, 31.1% C, and 5.43% H, these amounts suggested a nearly complete exchange of the nitrate for ibuprofen. The negligibly small amount of nitrogen (0.06%) and the similarity between the theoretical and observed percentages of carbon provided proof for the successful exchange and the absence of carbon dioxide intercalation. For every gram of LDH Ibu, 0.409 g corresponded to ibuprofen.

Dispersion of LDH Ibu in the PLLA matrix

When LDH Ibu was dispersed in the PLLA matrix, there was a slight additional intercalation of PLLA between the nanofiller layers, which resulted in a shift to a lower 2θ of the (003) reflection peak and increased *d*-spacing, as shown in Figure 2 and Table II. The TEM micrographs of the PLLA/LDH Ibu nanocomposites are shown in Figure 3(A–C), and intercalated and exfoliated structures of the LDH Ibu component were observed. The images were analyzed with Image-J (Java-based online image processing program developed by National Institutes of Health, Bethesda, Maryland). The dark lines were sections of the LDH Ibu layers about 1.3–1.5 nm thick. The distance between each dark line had an average distance of 14–17 nm. It was clear, however, that the localized structure showed an intercalated/exfoliated dispersion and that aggregation and clustering of the intercalated/exfoliated regions existed. Thus, the uniform dispersion of LDH Ibu in the PLLA matrix was limited as the nanofiller concentration increased.

Thermal stability

The TGA curves of the neat PLLA, LDH Ibu, Ibu, and PLLA/LDH Ibu nanocomposites and their first derivative plots [derivative thermogravimetry (DTG)] are shown in Figure 4(A,B), respectively. The thermal stability of the samples showed weight loss behavior as a function of temperature. For pure Ibu, the TGA curve displayed two weight loss zones and a total weight loss of nearly 80%. As shown by the DTG curve, the lower temperature weight loss zone centered at 80°C corresponded to the loss of water whereas the higher temperature one centered at 475°C corresponded to the ioss of ibuprofen. The TGA curve of the LDH Ibu sample indicated 50% weight loss, which corresponded well with the theoretical loss of water, the interlayer anion (ibuprofen), and the formation of a mixture of ZnO and $ZnAl_2O_4$ residue. The residue was black, which indicated the presence of some carbonaceous char. The DTG trace showed two bimodal weight loss zones centered around 100 and 190°C, respectively, and a single one centered at 450°C. The weight loss zone at 100°C was due to the evaporation of water molecules, both physically adsorbed and chemically bound, whereas those at 190 and 450°C were attributed to the collapse of hydroxide layers and the decomposition of the ibuprofen anion into gaseous CO_2 and H_2O, respectively. The presence of only three distinct

TABLE II
Effect of PLLA on the (003) Reflection Peak of LDH Ibu Showing an Intercalated Structure

Sample	2θ (°)	*d* (Å)	fwhm
LDH NO_3	9.80	9.01	0.23
LDH Ibu	3.84	22.95	0.69
1LDH Ibu	3.17	27.82	0.48
3LDH Ibu	3.15	27.99	0.81
5LDH Ibu	3.25	27.16	0.62

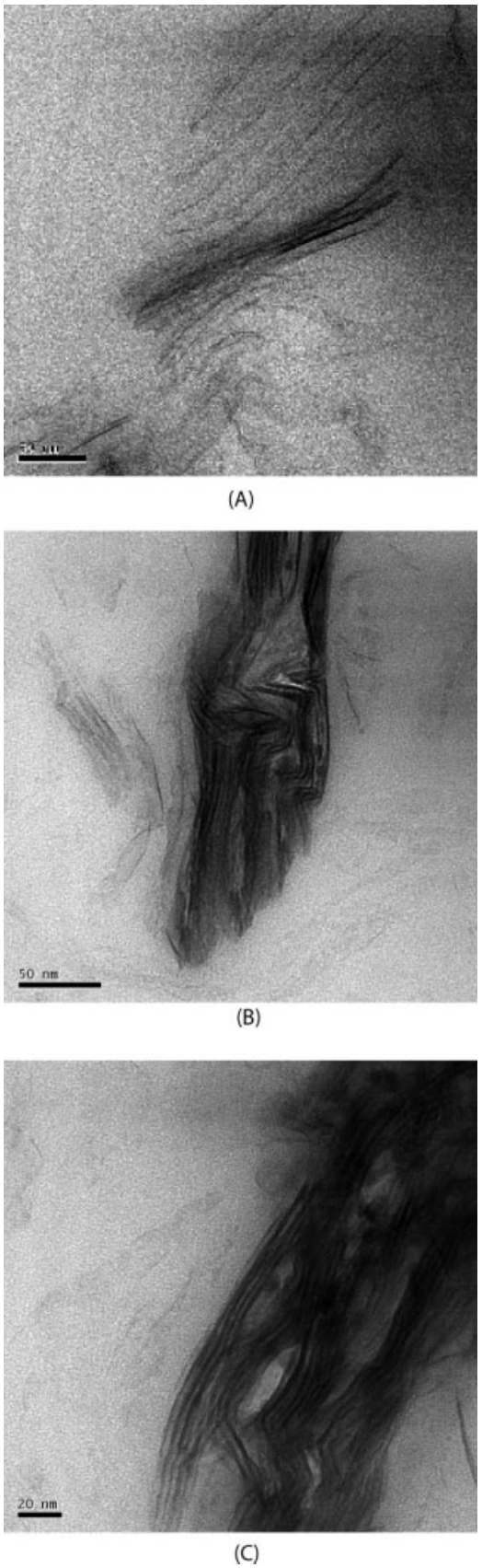

Figure 3 TEM micrographs of the PLLA/LDH Ibu nanocomposites: (A) 1LDH Ibu, (B) 3LDH Ibu, and (C) 5LDH Ibu.

thermal decomposition steps, of which two corresponded to the loss of water and the collapse of hydroxide layers, suggested that there was only one interlayer anion (which corresponded to the only remaining step), and hence, the exchange could be considered nearly complete.

The thermal degradation of PLLA is very complex and includes intramolecular transesterification leading to lactic acid and cyclic oligomers, cis-elimination leading to acrylic acid oligomers, and fragmentation producing acetaldehyde and carbon dioxide.[27] The DTG curve of PLLA showed two single weight loss zones centered at 120 and 387°C, respectively. The lower temperature weight loss zone corresponded to the moisture content (<3%), whereas the higher temperature one was attributed to the temperature of maximum decomposition (T_P) of PLLA. Indeed, pure PLLA started degrading at about 285°C and completely decomposed (0 wt %

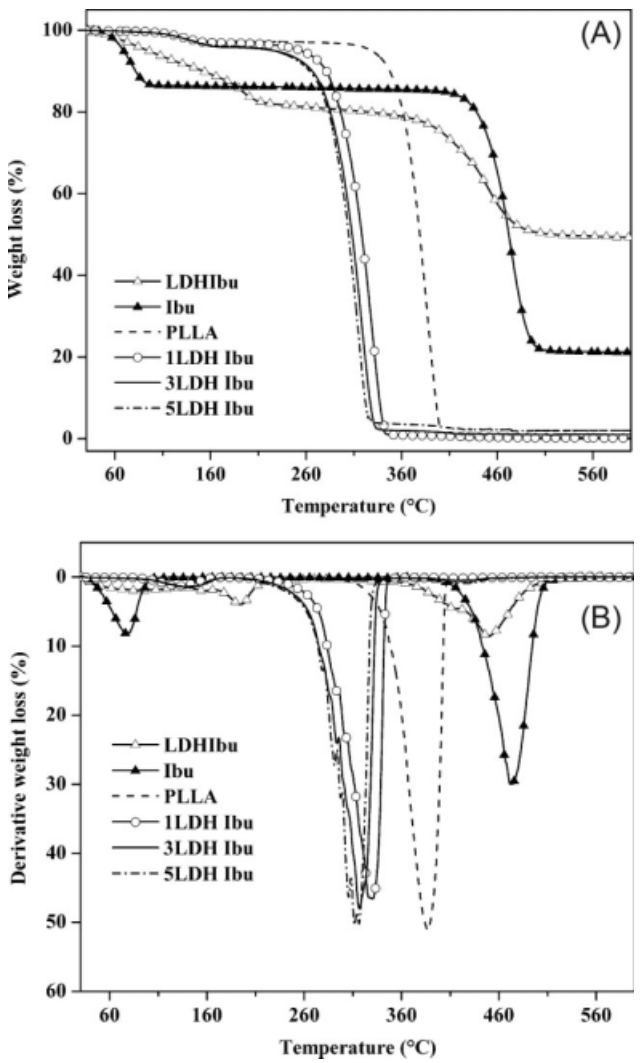

Figure 4 (A) TGA and (B) DTG traces of the neat LDH Ibu, neat Ibu, neat PLLA, and PLLA/LDH Ibu nanocomposites.

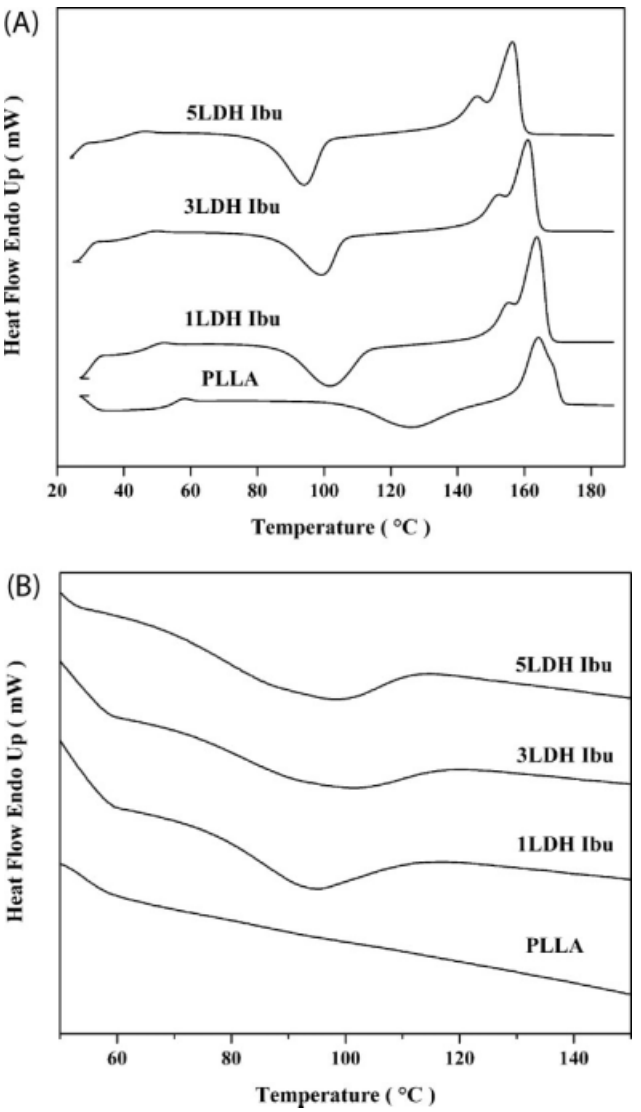

Figure 5 (A) DSC traces for the second heating of the neat PLLA and its nanocomposites, showing the effect of LDH Ibu on T_g, T_{cc}, and T_m and (B) DSC traces for the cooling of the neat PLLA and its nanocomposites, showing the melt-crystallization-promoting effect of LDH Ibu on the neat PLLA.

char residue) around 430°C. For the PLLA/LDH Ibu nanocomposites, the shape of the TGA curves was very similar to that of the parent PLLA, although the temperature of the decomposition step was lower. From the DTG curves, T_P decreased from 387°C for pure PLLA to 331, 317, and 311°C for 1LDH Ibu, 3LDH Ibu, and 5LDH Ibu, respectively, which indicated the decrease in the thermal stability of the neat PLLA with increasing LDH Ibu content. This behavior was due to the fact that the increase of the LDH Ibu loading thermally destabilized the polymer matrix, which thus decreased T_P. This behavior was due to the fact that LDH Ibu degradation was accompanied by water loss, which accelerated the PLLA hydrolytic decomposition. Therefore, we might have concluded that the PLLA/LDH Ibu interfaces were possible weak points of the nanocomposites. The thermal degradation of our nanocomposites left between 0.3–2% residue. Assuming that PLLA was completely volatilized and the ibuprofen anions were degraded, we regarded the weight residue remaining after 550°C as the real carbonaceous char content.

Thermal transitions

The effect of the addition of LDH Ibu on the thermal transitions of PLLA was investigated by DSC [Figs. 5(A,B)]. The glass-transition temperature (T_g), heat capacity (ΔC_p), melting temperature (T_m), melting enthalpy (ΔH_m), cold crystallization temperature (T_{cc}), cold crystallization enthalpy (ΔH_{cc}), melt crystallization temperature (T_{mc}), melt crystallization enthalpy (ΔH_{mc}), and degree of crystallinity (X_c) were obtained from the thermograms. The thermal properties of the cooling and second heating curves are summarized in Table III.

The thermal transitions of PLLA in composite systems have been widely investigated.[27–30] As shown in Figure 5(A), neat PLLA showed a T_g around 54.3°C, T_{cc} at 125.7, and T_m at 164.2 on heating. T_g decreased with increasing LDH Ibu concentration. It decreased from 54.3°C for pure PLLA to 47.0, 43.9, and 40.1°C for 1LDH Ibu, 3LDH Ibu, and 5LDH Ibu, respectively. Fujimori et al.[31] found that the T_g values of drawn PLLA/clay hybrid films slightly decreased with an increase in the clay concentration, which suggested that the free alkyl ammonium ion may associate with PLLA chains and play a role in plasticizing the PLLA matrix. Thus, the decrease observed in our nanocomposites could have been due to the plasticizing effect of the corresponding

TABLE III
Thermal Properties of the Cooling and Second Heating of PLLA and PLLA/LDH Ibu Nanocomposites

Sample	T_g (°C)	ΔC_p (J g^{-1} °C^{-1})	T_{cc} (°C)	ΔH_{cc} (J/g)	T_m (°C)		ΔH_m (J/g)	χ_c (%)	T_{mc} (°C)	ΔH_{mc} (J/g)
PLLA	54.3	0.674	125.7	−37.3	—	164.2	39.5	29.3	—	—
1LDH Ibu	47.0	0.564	101.7	−41.4	154.8	163.8	60.4	45.2	93.7	−9.0
3LDH Ibu	43.9	0.397	99.1	−33.8	152.0	161.0	54.0	41.2	96.7	−10.1
5LDH Ibu	40.1	0.386	94.0	−30.0	145.3	156.4	51.2	39.9	98.1	−11.2

ibuprofen anions. Likewise, ΔC_p decreased with increasing LDH Ibu content. With respect to the neat polymer, the PLLA/LDH Ibu nanocomposites showed double endothermic melting points, which shifted to lower temperature with increasing content of the nanofiller. The decrease in the melting points could have indicated an increase in the lamellar thickness. These peaks could have corresponded to the T_m of the crystalline phases and suggested the presence of two crystalline phases in the samples, and the fraction of the two ΔH_m reflected the relative amount of the crystalline phases in the PLLA/LDH Ibu nanocomposites. The values of ΔH_m in the nanocomposites were higher than that of the pure PLLA. However, in the PLLA/LDH Ibu nanocomposites, ΔH_m decreased with increased LDH Ibu content. The equilibrium heat of fusion of PLLA used to calculate X_c was 135 J/g.[31] X_c increased by 54, 41, and 36% for 1LDH Ibu, 3LDH Ibu, and 5LDH Ibu, respectively, with respect to that of the neat polymer. The increase in X_c coupled to the decrease in melting point implied that, although the lamella thickness increased, the crystal density also increased. On the other hand, T_{cc} showed a significant decrease when the nanofiller was added. It decreased from 125.7°C for the neat PLLA to 101.7, 99.1, and 94.0°C for 1LDH Ibu, 3LDH Ibu, and 5LDH Ibu, respectively. In the context of peak area, the neat PLLA showed a noticeable broad cold crystallization peak, which became narrow and smaller with increasing LDH Ibu content. The decrease in T_{cc} with increasing nanofiller content could have indicated some degree of faster crystallization rate in the PLLA/LDH Ibu nanocomposites. The change in the crystallization rate was further proved by analysis of the nonisothermal crystallization curves.

The T_{mc} values during the dynamic cooling were analyzed as a function of the concentration of LDH Ibu [Fig. 5(B)]. The cooling thermograms of the samples showed that the parent PLLA did not reveal any T_{mc} exotherm peak. The PLLA/LDH Ibu nanocomposites, however, did. A PLLA broad but shallow melt recrystallization peak was observed with the addition of LDH Ibu. For 1LDH Ibu, 3LDH Ibu, and 5LDH Ibu, T_{mc} peaked at 93.7, 96.7, and 98.1, respectively, which indicated a slight increase in the T_{mc} with increased nanofiller content. Usually, a lower T_{cc} indicates faster crystallization, whereas a lower T_{mc} indicates slower crystallization. Therefore, the decrease in T_{cc} coupled with the increase in T_{mc} could have been an indicator of a crystallization-promoting effect of the nanofiller.

Thermomechanical and mechanical properties

Figure 6 shows the relaxation spectrum in terms of storage modulus (E') and the loss tangent (tan δ) versus temperature at a frequency of 1 Hz for the virgin PLLA and its nanocomposites samples. E' represents the stiffness of a viscoelastic material and is proportional to the energy stored during a loading cycle. On the other hand, tan δ is defined as the ratio of loss modulus to E'. It is a measure of the energy lost, expressed in terms of recoverable energy, and represents mechanical damping or internal friction in a viscoelastic system.

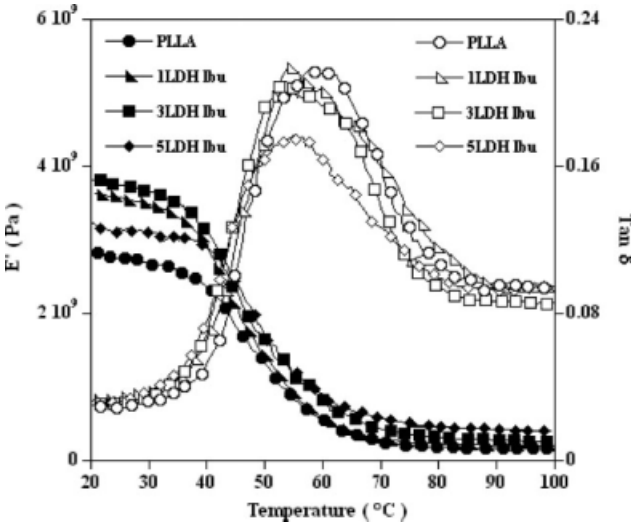

Figure 6 E' (solid markers) and tan δ (open markers) curves of the virgin PLLA and PLLA/LDH Ibu nanocomposites, showing an increase in E' and a slight shift to the lower temperatures of the tan δ peak.

As shown in the E' spectra, the nanocomposites films showed higher E' values than the virgin PLLA. The higher E' values of the PLLA/LDH Ibu nanocomposites reflected the reinforcement potential of the nanofiller in the biopolymer matrix. The increase in rubbery modulus was ascribed to the reinforcing effect of the nanofiller. Although E' generally increased with increasing LDH Ibu content, the 5LDH Ibu sample showed an E' less than those of the 1LDH Ibu and 3LDH Ibu samples. The decrease in E' of the 5LDH Ibu sample was attributed to increased aggregate formation, which led to a decrease in the mechanical properties. T_g of the virgin polymer obtained from the maximum tan δ curve was also affected with the addition of the nanofiller. In fact, neat PLLA showed a tan δ peak around 58°C, and a slight shift to lower temperatures was observed for all of the nanocomposites samples. These results were consistent with the DSC results. The decrease in the tan δ peak was attributed to the mobility of the amorphous chains promoted by the nanofiller.

The increase in E' was also supported by the increased mechanical properties indicated by tensile testing (Fig. 7 and Table IV). The addition of nanofiller resulted in 24, 32, and 16% increases in the elastic modulus (E) for 1LDH Ibu, 3LDH Ibu, and 5LDH

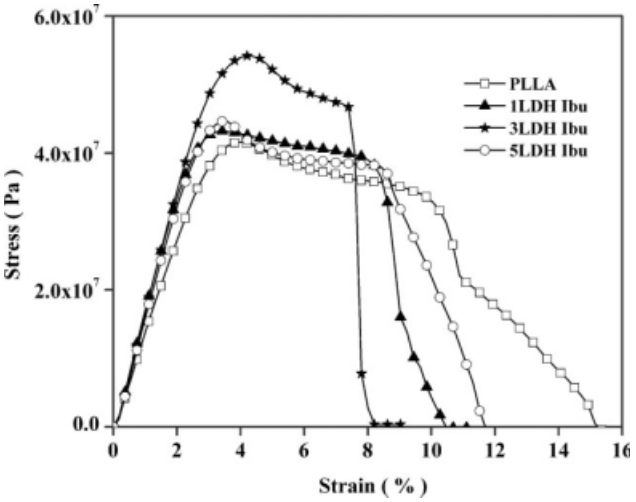

Figure 7 Tensile testing results for the neat PLLA and PLLA/LDH Ibu nanocomposites, showing an increase in UTS and Young's modulus and a decrease in the strain to failure with increasing LDH Ibu concentration.

Ibu, respectively. The ultimate tensile strength (UTS) followed the same trend observed for *E*. The UTS increased from 41.6 MPa for the virgin PLLA to 43.2, 54.2, and 44.6 MPa with the addition of 1, 3, and 5 wt % LDH Ibu, respectively. This increase indicated a synergistic effect of the nanofiller content on the tensile properties of the PLLA matrix and was attributed to a high degree of dispersion of the nanoplatelets within the biopolymer matrix, which led to a strong interaction between the biopolymer and the LDH. Although *E* and UTS generally increased with the addition of the nanofiller, the decrease in the *E* and UTS values of the 5LDH Ibu sample were explained by the formation of aggregates, which resulted in decreased mechanical properties because of decreased flow stress. Finally, the hybrids showed a decrease in the strain at break with increasing LDH Ibu content, which indicated an alteration in the plastic deformation of the PLLA matrix with the incorporation of the nanofiller.

Reduction in cell proliferation and release profile of ibuprofen

The SMC proliferation study was conducted on the surface of various samples, and glass and PLLA

TABLE IV
Mechanical Properties of the PLLA and PLLA/LDH Ibu Nanocomposites Showing Increases in *E* and UTS but Decreases in the Strain to Failure

Sample	*E* (GPa)	UTS (MPa)	Strain to failure (%)
PLLA	1.31 ± 0.09	41.6 ± 0.21	15.1 ± 0.40
1LDH Ibu	1.62 ± 0.05	43.2 ± 0.15	10.5 ± 0.35
3LDH Ibu	1.73 ± 0.04	54.2 ± 0.12	8.2 ± 0.75
5LDH Ibu	1.52 ± 0.06	44.6 ± 0.23	11.7 ± 0.15

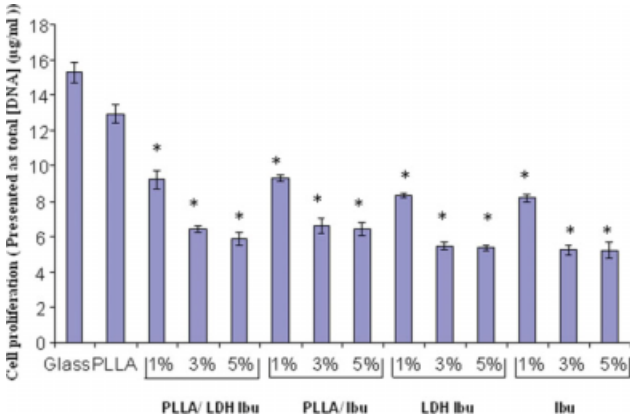

Figure 8 LDH Ibu blended PLLA films' reduced SMC proliferation. The cells were cultured in glass vials (control) or PLLA, PLLA/LDH Ibu, PLLA/Ibu, LDH Ibu, or Ibu samples with Ibu concentrations of 1, 3, and 5%. Cell proliferation was estimated with DNA assays as described in the Experimental section ($n = 4$; *significant difference in comparison with PLLA, $p < 0.05$). [Color figure can be viewed in the online issue, which is available at www.interscience.wiley.com.]

were used as controls. Samples with and without PLLA prepared with 1, 3, or 5% LDH Ibu or Ibu were also examined. Similar to previous studies, our results show that the cells did not grow well on PLLA surfaces compared to glass surfaces (Fig. 8; $n = 4$, $p < 0.05$). PLLA with 1 wt % LDH Ibu reduced cell proliferation significantly compared to PLLA alone. A plateau was formed for 3 and 5 wt % LDH Ibu in PLLA films. This plateau indicated that the inhibition was dose dependent and that the effective concentration for cell growth inhibition was between 3 and 5 wt %. The same behavior was observed when PLLA Ibu was used. However, the cell proliferation was significantly lower when LDH Ibu and Ibu were used without PLLA. This might have been due to the higher availability of Ibu without PLLA in comparison to Ibu blended with PLLA. The availability of Ibu depended on PLLA degradation, which limited the Ibu released in the media at each time point. The inhibition of SMC proliferation observed in our studies was solely due to Ibu because we observed that the growth of cells on either PLLA with LDH Ibu or LDH samples without Ibu was similar to that of the controls (results not shown).

To determine the release profile of Ibu from the nanocomposite films, we conducted drug-release studies with HPLC. The ibuprofen drug-release profiles are shown in Figure 9. The drug release followed a conventional two-stage elution profile, with a quick release (the first 15 h) followed by a slower release (up to 50 h). The initial fast rate of release was due to the diffusion of the absorbed drug from the surfaces of the LDH into the solution. A

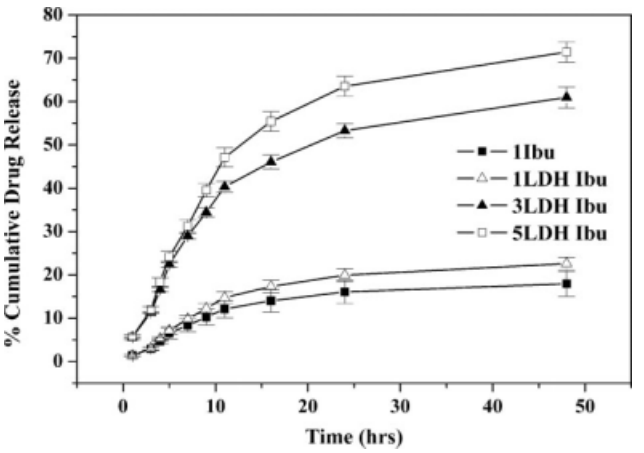

Figure 9 Cumulative drug-release (%) curves of PLLA modified with 1 wt % Ibu, 1LDH Ibu, 3LDH Ibu, and 5LDH Ibu.

modified Freundlich plot (diffusion kinetic model) gave a linear relationship (R^2 = 0.96–0.97) for the whole data that suggested that the release of ibuprofen was diffusion controlled (similar to the mechanism proposed for drug release from MgAl LDH functionalized with heparin[32]). This could have been due to the small dimensions of the LDH particles, which provided short diffusion paths for the Ibu to be released. The percentage cumulative drug release increased with the amount of ibuprofen in the nanocomposites: 5LDH Ibu > 3LDH Ibu > 1LDH Ibu > 1Ibu (1Ibu = 1 wt % ibuprofen in PLLA). Thus, the cell proliferation results complemented the results of the drug release, which indicated decreased cell proliferation in samples of higher released Ibu. Noting that 1 g of LDH Ibu had 0.409 g of ibuprofen, we compared the drug-release profile of the PLLA with the 1 wt % ibuprofen sample to the 1LDH Ibu, which contained 0.409 wt % ibuprofen. The drug release was quicker in the nanocomposites. Thus, LDH facilitated the release of the ibuprofen from PLLA. The findings correlated with decreased cell proliferation in PLLA modified with LDH Ibu compared to the PLLA/Ibu samples. Thus, LDH worked synergistically to strengthen PLLA, facilitated drug release, and decreased cell proliferation. The results indicate ranges of release complementary to prior work with ibuprofen. Ibuprofen has been shown to inhibit vascular SMC proliferation in a dose-dependent manner[33] through a cell cycle arrest (G0/G1 arrest). Ibuprofen has also been shown to reduce SMC proliferation by both cycloxygenase-dependent and cycloxygenase-independent pathways. A major advantage of ibuprofen is that this drug can be used at very high doses without any cytotoxicity effect.[33,34] Prior work has shown that the release of ibuprofen at much higher doses (>10 wt %) ranges from 10 to 80%, depending on the materials in these reports and studies.[35–37] Thus, using ibuprofen on LDH and dispersing the subsequent LDH in biopolymers facilitates drug release in deployable forms (films) and increases the mechanical performance of the biopolymer.

CONCLUSIONS

Simultaneous increases in the mechanical performance and inhibition of vascular SMC proliferation in PLLA were possible through the use of LDHs functionalized by nonsteroidal anti-inflammatory drugs such as ibuprofen. WAXD and TEM results indicate that an intercalated/exfoliated dispersion ensued. LDH Ibu did influence the thermal transitions of PLLA and acted as a nucleating agent by promoting the melt crystallization of the polymer. The overall crystallinity increased when the nanofiller was added. Decreased degradation temperatures were obtained when the LDH Ibu was introduced into the PLLA matrix. Increased moduli and UTS properties were obtained with increased LDH Ibu concentration. LDH Ibu incorporated in PLLA inhibited the proliferation of SMCs after 5 days of exposure. By comparing Ibu, PLLA/Ibu, and LDH functionalized with ibuprofen incorporated into PLLA, we concluded that the ibuprofen component was the dominant cause of the decreased cell proliferation. Incorporating ibuprofen into the LDH resulted in effective drug release, which led to a multibiofunctional nanocomposite with a significant mechanical advantage.

References

1. Törmälä, P.; Pohjonen, T.; Rokkanen, P. Proc Inst Mech Eng 1998, 212, 101.
2. Chu, C. C. In Biomedical Engineering Handbook; Bronzino, J. D., Ed.; CRC: Boca Raton, FL, 1995; p 611.
3. Rokkanen, P. U.; Böstman, O.; Hirvensalo, E.; Mäkelä, E. A.; Partio, E. K.; Patiala, H.; Vainionpaa, S.; Vihtonen, K.; Tormala, P Biomaterials 2000, 21, 2607.
4. Stancari, F.; Zanni, B.; Bernardi, F.; Calandriello, M.; Salvatorelli, G. Quintessenz 2000, 51, 47.
5. Athanasius, K. A.; Agrawal, C. M.; Barber, A.; Burkhart, S. Arthroscopy 1998, 7, 726.
6. Datta, R.; Tsai, S. P.; Bonsignore, P.; Moon, S. H.; Frank, J. R. FEMS Microbiol Rev 1995, 16, 221.
7. Vert, M.; Schwarch, G.; Coudane, J. J Macromol Sci Pure Appl Chem 1995, 32, 787.
8. Lunt, J. Polym Degrad Stab 1998, 59, 145.
9. Goldberg, M. J Biomater Sci 2007, 18, 241.
10. Guan, Y. T.; Li, Y.; Jin, Z. H. J Bioact Compat Polym 2006, 21, 445.
11. Mohanambe, L.; Vasudevan, S. J Phys Chem B 2005, 109, 15651.
12. Gordijo, C. R.; Barbosa, C. A. S.; Ferreira, D. C. A. M.; Costantino, V. R. L.; Silva, O. D. D. J Pharm Sci 2005, 94, 1135.
13. Ambrogi, V.; Fardella, G.; Grandolini, G.; Perioli, L.; Tiralti, M. C. AAPS Pharm Sci Technol 2002, 3, 1.

14. Choy, J. H.; Kwak, S. Y.; Jeong, Y. J.; Park, J. S. Angew Chem Int 2000, 39, 4041.
15. Khan, A. I.; Lei, L.; Norquist, A. J.; O'Hare, D. Chem Commun 2001, 22, 2342.
16. Choy, J. H.; Jung, J. S.; Oh, J. M.; Park, M.; Jeong, J.; Kang, Y. K.; Han, O. J. Biomaterials 2004, 25, 3059.
17. Lee, J. H.; Park, T. G.; Park, H. S.; Lee, D. S.; Lee, Y. K.; Yoon, S. C.; Nam, J. D. Biomaterials 2003, 24, 2773.
18. D'Souza, N. A.; Strauss, R. A.; Hernandez-Luna, A.; Sahu, L. In Handbook of Polymer Processing; Harper, C., Ed.; Wiley: New York, 2006.
19. Braterman, P. S.; Xu, Z. P.; Yarberry, F. In Handbook of Layered Materials; Auerbach, S. M.; Carrado, K. A.; Dutta, P. K., Eds.; Marcel Dekker: New York, 2004; p 373.
20. Layered Double Hydroxides: Present and Future; Rives, V., Ed.; Nova Science: New York, 2001; p 1.
21. (a) Whittingham, M. S.; Jacobson, A. J. Intercalation Chemistry; Academic Press: New York, 1982; (b) Alberti, G.; Costantino, U. In Comprehensive Supramolecular Chemistry; Alberti, G.; Bein, T., Eds.; Wiley: Chichester, England, 1996; vol. 7, p 1.
22. Qui, L.; Chen, W.; Qu, B. Polym Degrad Stab 2005, 87, 433.
23. Ambrogi, V.; Fardella, G.; Grandolini, G.; Perioli, L. Int J Pharm 2001, 220, 23.
24. Hwang, S. H.; Han, Y. S.; Choy, J. H. Bull Korean Chem Soc 2001, 22, 1019.
25. Hussein, M. Z.; Zainal, Z.; Yahaya, A. H. J Controlled Release 2002, 82, 417.
26. Xu, Z. P.; Braterman, P. S. J Mater Chem 2003, 13, 268.
27. Andricic, B.; Kovacic, T.; Perinovic, S.; Grgic, A. Macromol Symp 2008, 263, 96.
28. Thellen, C.; Orroth, C.; Froio, D.; Ziegler, D.; Lucciarini, J.; Farrell, R.; D'Souza, N. A.; Ratto, J. A. Polymer 2005, 46, 11716.
29. Marras, S. I.; Zuburtikudis, I.; Panayiotou, C. Eur Polym J 2007, 43, 2191.
30. Moon, S.; Iji, M. J Polym Sci Part A: Polym Chem 2008, 46, 4433.
31. Fujimori, A.; Ninomiya, N.; Masuko, T. Polym Adv Technol 2008, 19, 1735.
32. Gu, Z.; Thomas, A. C.; Xu, Z. P.; Campbell, J. H.; Lu, G. Q. Chem Mater 2008, 20, 3715.
33. Weber, A.; Yildirim, H.; Schror, K. Eur J Pharm 2000, 389, 67.
34. Brooks, G.; Yu, M.; Wang, Y.; Crabbe, M. J. C.; Shattock.; M. J.; Harper, J. V. J Pharm Pharmacol 2003, 55, 519.
35. Lee, J. H.; Go, A. K.; Oh, S. H.; Lee, K. E.; Yuk, S. H. Biomaterials 2005, 26, 671.
36. Vallet-Regi, M.; Granado, S.; Arcos, D.; Gordo, M.; Cabanas, M. V.; Ragel, C. V.; Salinas, A. J.; San Roman, J. J Biomed Mater Res 1998, 39, 423.
37. Gallardo, A.; Eguiburu, J. L.; Fernandez Berridi, M. J.; San Roman, J. J Controlled Release 1998, 55, 171.